Comparison of the statolith structures of *Chironex fleckeri* (Cnidaria, Cubozoa) and *Periphylla periphylla* (Cnidaria, Scyphozoa): a phylogenetic approach

Authors: Sötje I[1], Neues F[2], Epple M[2], Ludwig W[3,4], Rack A[3], Gordon M[5], Boese R[2], Tiemann H[1]

[1]Biocenter Grindel and Zoological Museum, University of Hamburg, Martin-Luther-King-Platz 3, 20146 Hamburg, Germany
[2]Inorganic Chemistry, University of Duisburg-Essen, Campus Essen, Universitaetsstraße 5-7, D-45117 Essen, Germany
[3]European Synchrotron Radiation Facility, BP220, F-38043 Grenoble Cedex, France
[4]Institut National des Sciences Appliquées de Lyon, 20, avenue Albert Einstein, F-69621 Villeurbanne Cedex, France
[5]School of Marine and Tropical Biology, James Cook University, McGregor Road, Smithfield QLD 4878, Australia

Please address all correspondence during handling of the manuscript to:
Dr. Ilka Sötje, Biocenter Grindel and Zoological Museum, University of Hamburg, Martin-Luther-King-Platz 3, 20146 Hamburg, Germany

Email ilka.soetje@zoologie.uni-hamburg.de
Phone +49 40 42838-5644
Fax +49 40 42838-3937

Abstract

The rhopalia and statocysts of *P. periphylla* and *C. fleckeri* were examined histologically and showed several homologous characteristics. Differences in sensory area distribution could be connected to a slightly different functionality of equilibrium sensing. In *P. periphylla*, the statoliths (crystals) grow independently of each other; whereas in *C. fleckeri*, one large crystal covers the smaller ones. The structures of both statoliths were examined in detail with single-crystal diffraction, microtomography and diffraction contrast tomography. The single compact statolith of *C. fleckeri* consisted of bassanite, as was previously known only for other rhopaliophoran medusae. An origin area with several small oligocrystals was located in the centre of the cubozoan statolith. The origin areas and the accretion of statoliths are similar in both species. Our results lead to the assumption that the single bassanite statolith of *C. fleckeri* (Cnidaria, Cubozoa) is a progression of the scyphozoan multiplex statolith. It is therefore suggested that the Cubozoa are derived from a scyphozoan ancestor and are a highly developed taxa within the Rhopaliophora.

Key words: *Chironex fleckeri*, *Periphylla periphylla*, Rhopaliophora, Cubozoa, Scyphozoa, phylogeny, rhopalium, statolith, bassanite

Introduction

Evident in the fossil records from the Middle Cambrian about 600 millions years ago, the Cnidaria are one of the oldest animal phyla (Coates 2003). Earliest fossils already displayed characteristics that are still present in the medusae of the recent taxa (Adler et al. 2007, Cartwright et al. 2007). Despite more than a hundred years of investigation, the phylogenetic tree and systematics of the Cnidaria is still subject to considerable discussion. At present, the most common division is into the four classes; Anthozoa, Scyphozoa, Cubozoa and Hydrozoa (Schuchert 1993, Werner 1993). Some authors have, however, introduced an additional class, the Staurozoa (Marques and Collins 2004), while others distinguish only three classes, grouping Cubozoa with Scyphozoa (Matsumoto 1995, Rupert et al. 2004). Only the three taxa, the Hydrozoa, Scyphozoa and Cubozoa develop pelagic medusa stages with marginal sense organs bearing statocysts (Russel 1970, Werner 1993). While the medusa stage could have developed once, twice or three times within the different taxa (Collins 2002, Salvini-Plawen 1978, Schuchert 1993, Thiel 1966, Werner 1973, 1993) the statocyst, which is crucial in medusae orientation, must have developed together with the pelagic stage.

The Scyphozoa and Cubozoa develop statocysts that generally contain biomineralic crystals (statoliths). Both taxa are combined as sister groups within the taxon Rhopaliophora because of similarities in the medusa formation and the development of marginal sense organs (rhopalia) from tentacles bases (Werner 1975, Straehler-Pohl and Jarms 2005). The formation of the hydrozoan medusa and its marginal sense organs are a divergent development, because of their origin as a depression in the velum (Ax 1995, Singla 1975, Werner 1993). Evidence for the differential origin of the marginal sense organs in Rhopaliophora and Hydrozoa is supported by a comparison of their statolith material composition. Statoliths of hydrozoans like *Obelia*, *Aglantha* and Trachylida are composed of calcium magnesium phosphate (Chapman 1985, Singla 1975), whereas statoliths of the rhopaliophoran medusae are composed of bassanite (calcium sulphate hemihydrate) (Becker et al. 2005, Tiemann et al. 2002, Tiemann et al. 2006), which has been described as gypsum in earlier publications (Chapman 1985, Pollmanns and Hündgen 1981, Spangenberg and Beck 1968, Ueno et al. 1995, Ueno et al. 1997, Vinnikov et al. 1981).

Although the statolith material composition is the same in all examined rhopaliophoran medusae, the structure of the scyphozoan and cubozoan statolith appears to differ. Scyphozoan statocysts mostly consist of an accumulation of single crystals (statoliths) (Arai 1997, Becker et al. 2005, Russell 1970, Spangenberg and Beck 1968), whereas grown cubozoan medusae bear a single large statolith within the statocyst (Chapman 1985, Gordon et al. 2004, Kawamura et al. 2003, Ueno et al. 1995, Ueno et al. 1997).

Classification using established morphological features is in occasional disagreement regarding the phylogenetic tree of the Cnidaria, when compared to classification methods utilising molecular data. Therefore, it is a matter of ongoing debate whether the class Cubozoa is a sister group of the Scyphozoa including the order Stauromedusae (Salvini-Plaven 1978, Schuchert 1993, Straehler-Pohl and Jarms 2005, Straehler-Pohl 2009, Werner 1973), or is a sister group of the Staurozoa and is, rather remotely, related to the remaining scyphozoans (Collins 2002, Collins et al. 2006, Marques and Collins 2004, Thiel 1966).

Details of statolith crystallographic structure are a useful additional tool when investigating the phylogenetic relationships amongst different taxa. To date, examinations of statoliths from several cubozoan species are mostly done with light-microscopic or scanning electron methods (Chapman 1985, Gordon et al. 2004, Ueno et al. 1995, Ueno et al. 1997). Therefore, information about the statolith crystal structure and formation is currently absent. In the present investigation, we used more sophisticated methods including single-crystal x-ray diffraction, microtomography and diffraction contrast tomography to examine and compare the statoliths of *Chironex fleckeri* Southcott, 1956 (Chirodropidae, Cubozoa) and *Periphylla periphylla* (Péron and Lesueur, 1809) (Coronatae, Scyphozoa).

Materials and methods

Chironex fleckeri medusae were collected by hand from the shallow (< 0.5 m) sandy foreshores of Hey Point (estuary site) and Wooldrum Point (coastal site), Weipa, Australia in 2007. The inter pedalia distance (IPD) of each medusa was measured to the nearest mm, taken to be the distance between the midline of alternate pedalia along the line passing through the rhopalia. The four rhopalia of each medusa were removed by pushing a cylindrical stainless steel tube of 15 mm diameter through the mesoglea surrounding the niche, and placed in 90 % ethanol. Individual statoliths were later dissected from the rhopalia using needle point tweezers, cleaned of all biological material and preserved in 90 % ethanol.

Morphological and histological examinations of *C. fleckeri* rhopalia were carried out on material from the "Lower Invertebrates I" collection of the Zoological Museum in Hamburg (No. C11193). The medusa was collected by hand by W. N. Hamner in 0.5 m depth at Townsville (Australia) in 1976 and was preserved in 4 % formaldehyde first and stored in 70 % ethanol thereafter. The IPD of the examined medusa was 33 mm. The rhopalia were dehydrated further using ethanol and embedded in paraplast with the intermedium benzylbenzoate. Sections (6 µm) were stained with nuclear fast-red-aluminium sulphate and light green-orange y (Adam and Czihak 1964).

Specimens of *P. periphylla* were collected with a conical ring-net, 2 m diameter with 500 µm mesh size (Fraser 1968) during cruises with RV Håkon Mosby in Lurefjord and Sognefjord (Norway). For rhopalia histological examination samples were taken during 1999 and for the statolith examinations during the years 2003 and 2004. Immediately after capture, the medusa coronal diameter (CD) was measured and the rhopalia were detached and fixed in 80 % ethanol for statolith examinations. Statocyst widths were measured and transferred into water-free glycerol on microscopic slides before the statoliths were separated from each other. All statoliths of one statocyst were counted, and widths of the five largest statoliths were measured with an eyepiece micrometre. Examinations were performed with Zeiss Neofluar objectives at 10-40-fold magnification.

The examined medusa of *P. periphylla* had a CD of 8.2 mm and a statocyst width of approximately 110 µm. For histological examination the rhopalia were preserved in 4 % formaldehyde/seawater solution immediately after collection. Preparation for light-microscopy was made by dehydration in acetone and embedding in Spurr (Robinson et al. 1985). Sections (0.5 µm) were stained with toluidine-blue-pyronin (Adam and Czihak 1964), examined with Zeiss Neofluar objectives and documented by photomicrographs or by drawing using a camera lucida.

The IPD of the examined *C. fleckeri* medusa was 98 mm and the examined statolith was 878 µm long and 464 µm wide. For single-crystal x-ray diffraction the statolith was mounted with instant adhesive on a thin glass fibre, which was attached to a brass pin and was mounted onto the heads of the goniometer. The single-crystal x-ray diffraction on *C. fleckeri* statoliths was carried out at the diffractometer Siemens SMART three axis goniometer with APEX II area detector system with a θ range of 3.38-29.44° and a completeness of 96.7 % (index ranges $9 \le h \le 9$, $-9 \le k \le 9$, $-7 \le l \le 8$). The diffractometer control software was Bruker AXS APEX 2 version 3.0/2009, which was also used for data reduction and empirical absorption correction. Structure solution and refinement was carried out with the Bruker AXS SHELXTL version 2008/4/© 2008 software.

For synchrotron x-ray microtomography (SRµ-CT) of both species and for x-ray diffraction contrast tomography (DCT) of *C. fleckeri* ethanol preserved statocysts respectively statoliths were dehydrated in acetone and embedded in Spurr medium (Robinson et al. 1985). The IPD of the examined *C. fleckeri* medusa was 135 mm and the examined statolith was 830 µm long and 444 µm wide.

The microtomography scans of the *P. periphylla* rhopalia were carried out at beamline BW2 at HASYLAB/DESY (Hamburg, Germany). The CDs of the different examined medusae were 8.4 mm and 55 mm and statocyst width 230 µm and 560 µm of in accordance. The synchrotron radiation was monochromatized to a) 10keV and b) 14keV. Projection images were recorded in steps of 0.25 from 0 to 180 degrees. The detector was a KX2 instrument (Apogee Instruments; 14-bit digitalization at 1.25 MHz, 1536·1024 pixel; each 9·9 μm^2). For normalization of the recorded data, flat field images of the beam were recorded every eight projections. Reconstruction was performed using a filtered backprojection algorithm (Donath et al. 2004). 3D renderings were created with the program VG Studio MAX 1.2. The voxel side length after reconstruction was 2.06 µm and 2.10 µm.

The microtomography scan of the *C. fleckeri* statolith was performed at the TopoTomo beamline of the ANKA light source (Karlsruhe, Germany) using polychromatic illumination (the radiation of the bending magnet source was filtered by a 1-mm-thick Si and a 0.5-mm-thick Be filter, resulting in a broad spectrum with the mean energy around 20 keV) (Rack et al. 2009). The detector employed consisted a visible-light microscope (OptiquePeter, France) equipped with a 4x Olympus objective (NA 0.16) and a 2.5x eye-piece. The microscope is used to project the luminescence image of a 25-µm-thick Eu-doped $Lu_3Al_5O_{12}$ (LAG:Eu) scintillating thin film (grown on top of a 150-µm-thick $Y_3Al_5O_{12}$ (YAG) substrate) onto a pco. 4000 CCD camera (PCO AG, Germany – 4008 x 2672 pixels, each 9 µm in size, 5000:1 dynamic range). The spatial resolving power of the detector is 2.5 µm (0.9 µm effective pixel size) (Rack et al. 2009). 1000 projection images were recorded within a 180° scan. Tomographic reconstruction was done utilizing the PyHST software package of the European Synchrotron Radiation Facility (Mirone et al. 2009). For the volume renderings, the software package myVGI 1.2 by Volume Graphics GmbH was employed.

The X-ray diffraction contrast tomography (DCT) scan of the *C. fleckeri* statolith was performed at beamline ID19 beamline of ESRF (Ludwig et al. 2008, Johnson et al. 2008, Ludwig et al. 2009). 360 monochromatic beam (17.6 keV) projection images, each integrated over 1 degree in rotation angle, were recorded on a high-resolution detector system (4.8 mm field of view; 2.4 µm pixel size), positioned 5 mm downstream the sample. The size of the X-ray beam was adjusted to about 1x1 mm, illuminating the entire sample at any rotation angle. From the corresponding direct beam absorption image formed in the central area of the detector screen one can calculate the conventional absorption contrast tomogram. Due to the proximity of sample and detector part of the diffracted beams are captured on the detector. These "diffraction spots" can be approximated as parallel projections of the grain. After background correction of the raw images, 380 such diffraction spots were segmented and used for further analysis. Out of the initial 380 spots 180 Friedel pairs (hkl and -h-k-l reflections) of diffraction spots were identified and unambiguously indexed into 10 distinct grains sets, using the unitcell parameters and spacegroup of "bassanite" (Abriel and Nesper 1993). Details of the polycrystal index and reconstruction process can be found in (Ludwig et al. 2009).

Results

<u>*Periphylla periphylla* and *Chironex fleckeri*: Morphology and histology of the rhopalia</u>

In *Periphylla periphylla* medusa, four rhopalia were present at the bell margin, hanging downwards between the clefts of marginal lappets. The rhopalium consisted of a proximal bulb and a distal statocyst composed of many refractive crystals (statoliths) (Figs. 1, 4a). The connection of the basal part of the rhopalium (bulb) and the statocyst were constricted and were provided with a thickened and compact mesogloea. The statocyst was covered by an epidermal hood which was situated in the area between the bulb and the statocyst. The epidermis of the hood was a cuboidal epithelium on the outer side and plate-like on the inner side, with the latter being differentiated at the base of the hood by a thickened sensory area. The sensory areas are characterized by non-motile kinocilia on their surface. The epidermis of the statocyst closely to the hood is differentiated into a cylindrical sensory area. A second, flatter sensory area existed on the opposite proximal side of the statocyst. The proximal side of the bulb of the rhopalium was differentiated into a pseudostratified epithelium (with neurons situated apically) and a neuropil. The gastrodermis of the bulb surrounded the gastrovascular cavity, whereas the statocyst was filled with gastrodermis completely. The gastrodermal cells contained many lipid droplets within the basal part of the rhopalium and contained the statolith vacuoles within the statocyst. The smallest statolith vacuoles were located towards the base of the statocyst.

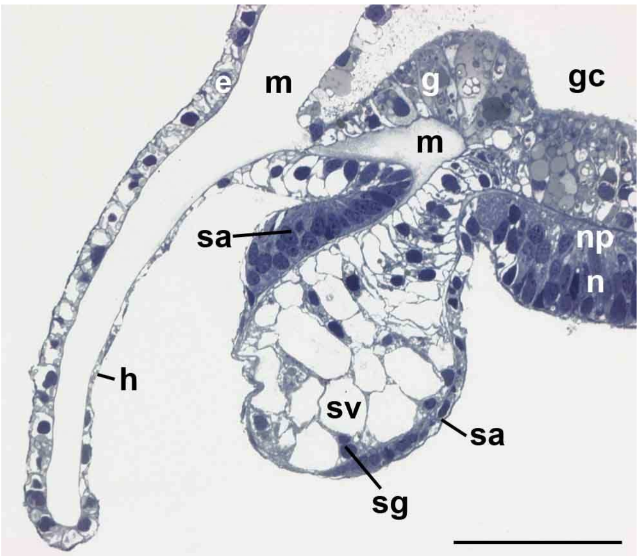

Fig. 1: *Periphylla periphylla*: Longitudinal section of the rhopalium, median, photograph, scale bar 100 µm, e-epidermis, g-gastrodermis, gc-gastrovascular cavity, h-hood, m-mesogloea, n-neurons, np-neuropil, sa-sensory area, sg-statolith producing gastrodermis, sv-statolith vacuole (statoliths are dissolved during preparation).

In *Chironex fleckeri* medusa, four rhopalia were present in epidermal niches located close to the bell margin, and alternating with four groups of tentacles. The rhopalia were connected to the roof of the rhopalial niche by a stalk. Each rhopalium had a compact structure, which included a statocyst distally and a basal section within which the eyes were housed (Figs. 2, 4b). The rhopalium had a compact structure, including the statocyst and the bulb that housed the eyes (Figs. 2, 4b). The epidermis of the statocyst region was differentiated into a sensory area on both sides. A gastrovascular cavity was located within the basal part of the rhopalium (Fig. 4). The epidermis of this region was differentiated to a pseudostratified epithelium with neurons and a subjacent neuropil. Balloon cells were apparent near the aboral lens eye. The gastrodermis of the statocyst enclosed one large region, which contained the statolith. The statocyst was broadly attached to rest of the rhopalium. The gastrodermal layer of the statocyst was enclosed by a thin mesogloeal layer, whereas the mesogloea was thicker and more compact in the aboral and distal part of the transition zone (Fig. 3).

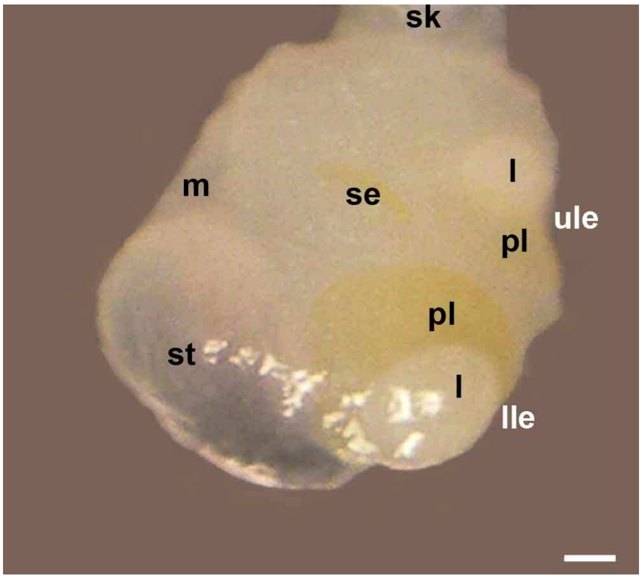

Fig. 2: *Chironex fleckeri*: lightmicroscopical photograph of a complete fixated (90 % ethanol) rhopalium, paramedian view, scale bar 100 µm, l-lense, lle-lower lens eye, m-mesogloea, pl-pigment layer, sk-stalk, se-slit eye, st-statolith, ule-upper lens eye.

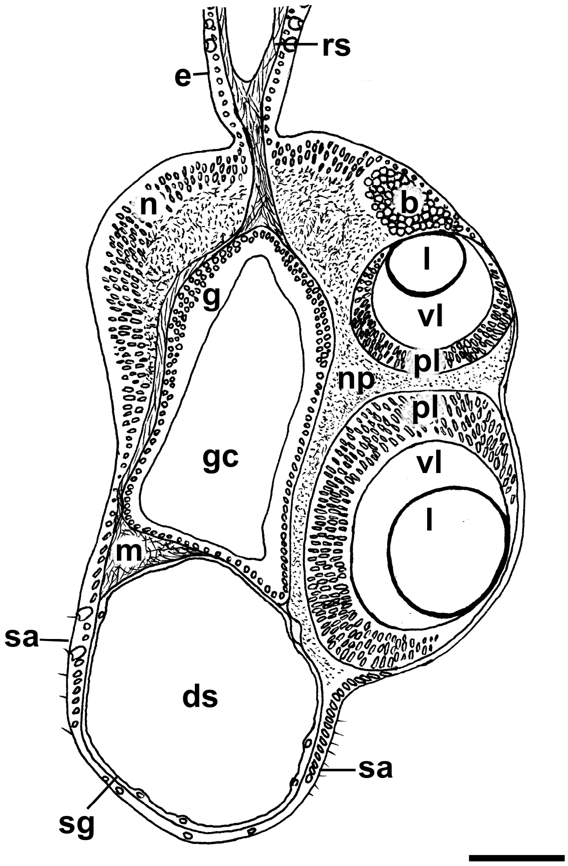

Fig. 3: *Chironex fleckeri*: Longitudinal section of the rhopalium, median, diagram, scale bar 100 µm, the gastrovascular channel within the stalk is not shown, b-balloon cells, l-lens, e-

epidermis, g-gastrodermis, gc-gastrovascular cavity, m-mesogloea, n-neurons, np-neuropil, pl-pigment layer, rs-rhopalial stalk, sa-sensory area, sg-statolith producing gastrodermis, ds-dissoved statolith , vl-vitrous layer.

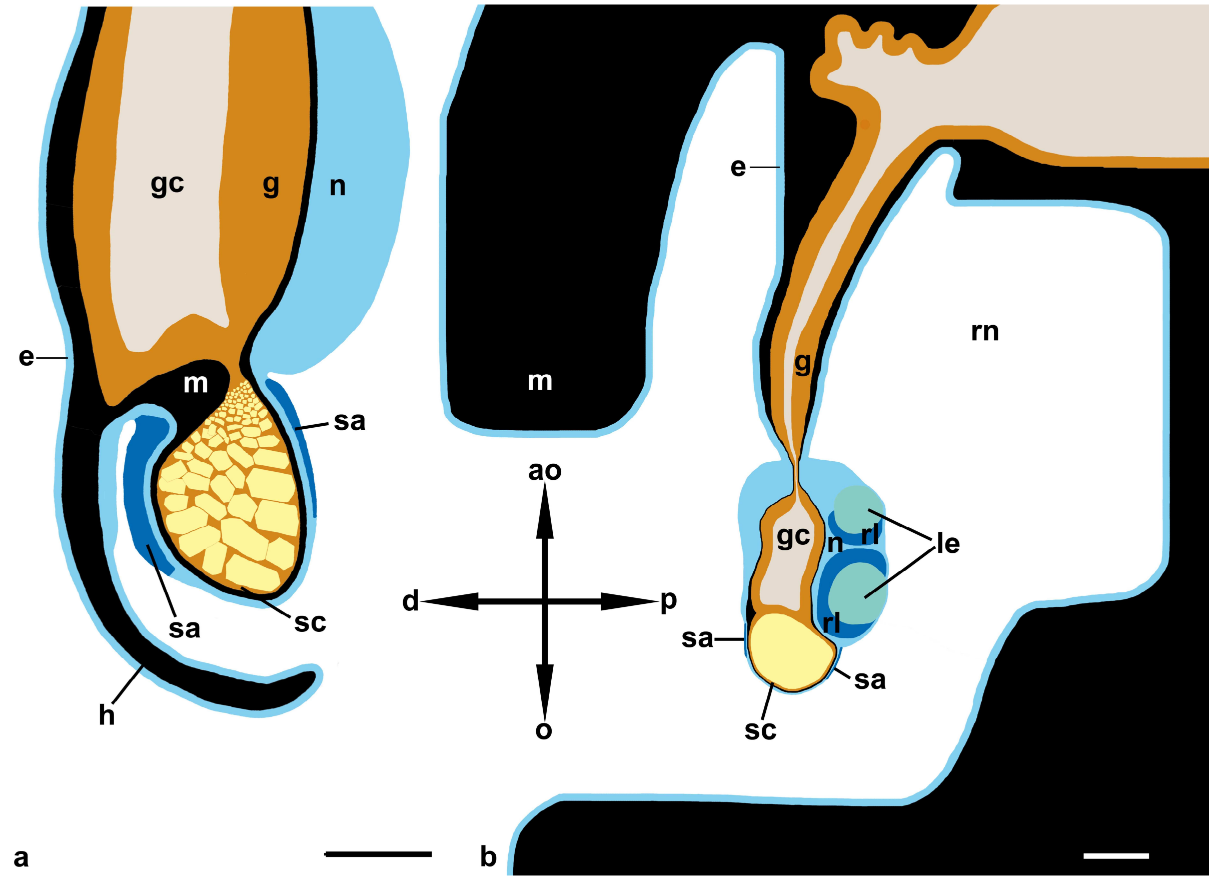

Fig. 4: Diagram of a longitudinal section through a rhopalium.
a *Periphylla periphylla*, scale bar 50 µm **b** *Chironex fleckeri* scale bar 200 µm
e-epidermis, g-gastrodermis, gc-gastrovascular cavity, h-hood, le-lens eye with retina, m-mesogloea, n-neuropil, rl- retinal layer, rn-rhopalial niche, sa-sensory area, sc-statocyst with statolith(s), rhopalium position (arrow cross): ao-aboral, d-distal, o-oral, p-proximal.

<u>*Periphylla periphylla*: Growth of statocysts and statoliths</u>

The growth of the statocyst as well as the number and growth of the statoliths were examined. Statocyst width (R^2 = 0.9443) as well as number of statoliths per statocyst (R^2 = 0.9755) increased exponentially with the growth of medusae (Fig. 5 a, b). The mean width of the five largest statoliths increased logarithmically with medusa growth (R^2 = 0.7095, Fig. 5c) (1.8-185 mm in diameter).

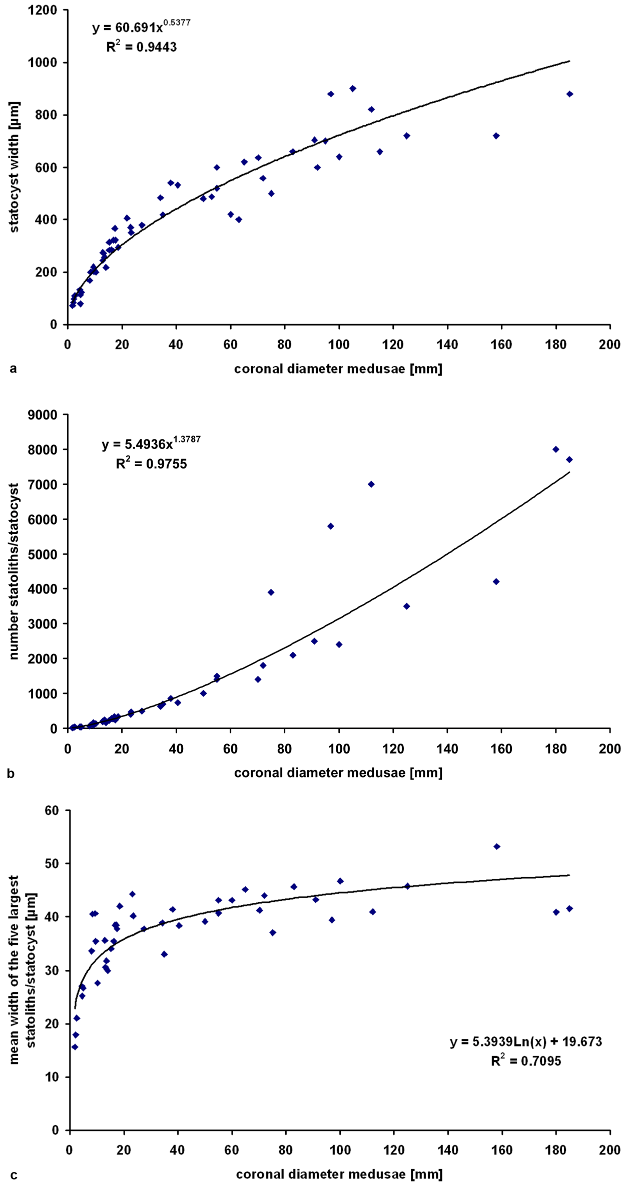

Fig. 5: *Periphylla periphylla*. **a** Increasing statocyst width in relation to medusa diameter, examined individuals n=56, **b** Increasing statolith number in relation to medusa diameter, examined individuals n=43, **c** Increasing statolith width in relation to medusa diameter, examined individuals n=45.

<u>*Chironex fleckeri*: X-ray single crystal diffraction</u>

The x-ray single crystal diffraction of the *C. fleckeri* statolith demonstrated that it consisted of several oligocrystals with minimum sizes of 50 µm. The crystal structure was completely clarified. The crystals were determined to be oligocrystals, because of the orientation of their crystal lattice in various axes. The statolith material consisted of calcium sulfate hemihydrate (bassanite) with an empirical formula Ca $SO_4 \cdot 0.50\ H_2O$ with a density of ρ (calc) of 2.711 g cm^{-3} at a temperature of T = 183(2) K. The structure of the mineral was confirmed to be bassanite in accordance with the crystallographic literature. The crystal shape was a plate with λ = 0.71073 Å and the crystal system is trigonal. The structural parameters of the trigonal cell unit dimensions (crystal system) were refined to a space group $P\ 3_1 21$ a = 6.95150(10), b = 6.95150(10) and c = 6.3516(3) Å and $\alpha = \beta$ = 90°, γ = 120°, V = 265.810(14) $Å^3$ (Z = 3).

<u>*Periphylla periphylla*: Microtomography scan (SRµ-CT) of the statocyst</u>

The microtomography scan showed the distribution of the statoliths within a rhopalium of *P. periphylla* (Fig. 6). The accumulation of statoliths within the statocyst had a helmet-like shape with an elongated area in the basal and oral part of the statocyst (Fig. 6 a+d). The basally and aborally located part appeared to be shorter. The apical area was rounded. The basally located area had a depression (arrows in figure 6 a, d, c, f) and contained the smallest crystals (Fig. 6 b+e). The largest crystals were located in the most apical part and in the apical periphery. Statoliths of intermediate size were located in the centre of the statocyst (Fig. 6 c+f). The arrangement of statoliths and the overall shape of the statolith accumulation did not change during the growth of the statocyst.

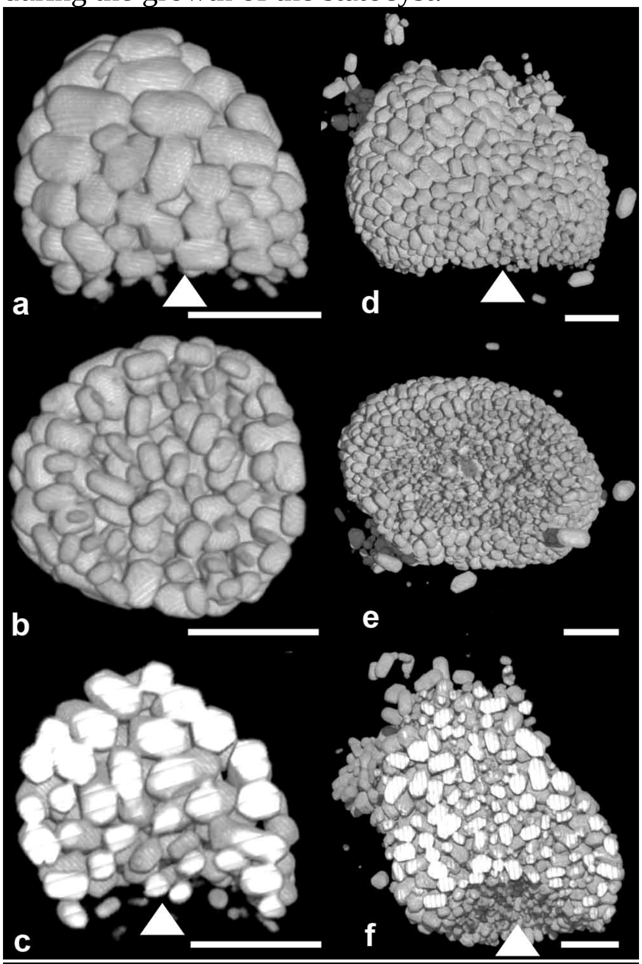

Fig. 6: *Periphylla periphylla*: Microtomography of statoliths of two statocysts from different sized medusae, **a-c** CD medusa 8.4 mm, **d-e** CD medusa 55 mm, **a-e** figures of the complete accumulation of statoliths of a statocyst, **a+e** side view, **b+e** view on the basal area containing the smallest statoliths, **c+f** longitudinal cut section through the reconstructed statocysts, arrows: basal area containing the smallest statoliths, scale bars 100 µm.

<u>*Chironex fleckeri*: Microtomography scan (SRµ-CT) of the statolith</u>

The statolith was solid and had an overall ellipsoid shape. A basally located V-shaped indentation ran parallel at 50 % of its shorter principal axis whereas the apical side was rounded. While the statolith surface was typically rough and granular, some areas were smooth and flattened (Fig. 7a). The cross-section through the shorter axis of the statolith reconstruction appeared homogenous. Granules could be seen at the marginal surface where some overgrowth of the statolith could also be seen (Fig. 7b).

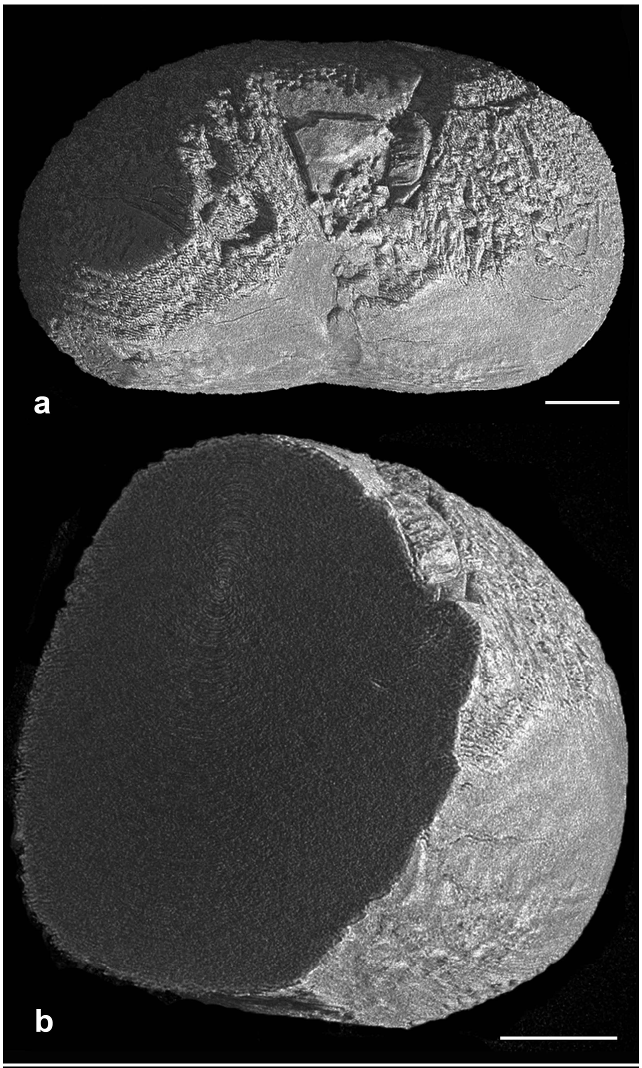

Fig. 7: *Chironex fleckeri*: Microtomography. **a** complete statolith, the lower side is directed towards the stalk (basally) **b** cut section through the reconstruction of the short axis of the statolith, scale bars 100 µm

Chironex fleckeri: Diffraction contrast tomography (DCT) of the statolith

The integrated, monochromatic beam projection images ("topographs") acquired during the DCT scan clearly show the presence of one large, dominant crystal, occupying about 85% of the entire volume of the statolith. Figure 8a shows one out of the twenty integrated, monochromatic beam projection images that have been acquired from this crystal. One can distinguish a radial structure which might indicate the presence of growth sectors diverging in different radial directions from a common point of origin, the supposed position of the initial crystal germ from which the statolith has grown. Figure 8b shows the diffraction CT reconstruction of the entire statolith and Figure 8c shows a cut through the diffraction CT reconstruction of the entire statolith, composed out of 9 distinct crystals. The shape and the 3D spatial arrangement of some of the smaller crystals resemble growth sectors too, but their distinct orientation suggests that these crystals have grown from distinct germs, located in the central region of the statolith (Fig. 8d).

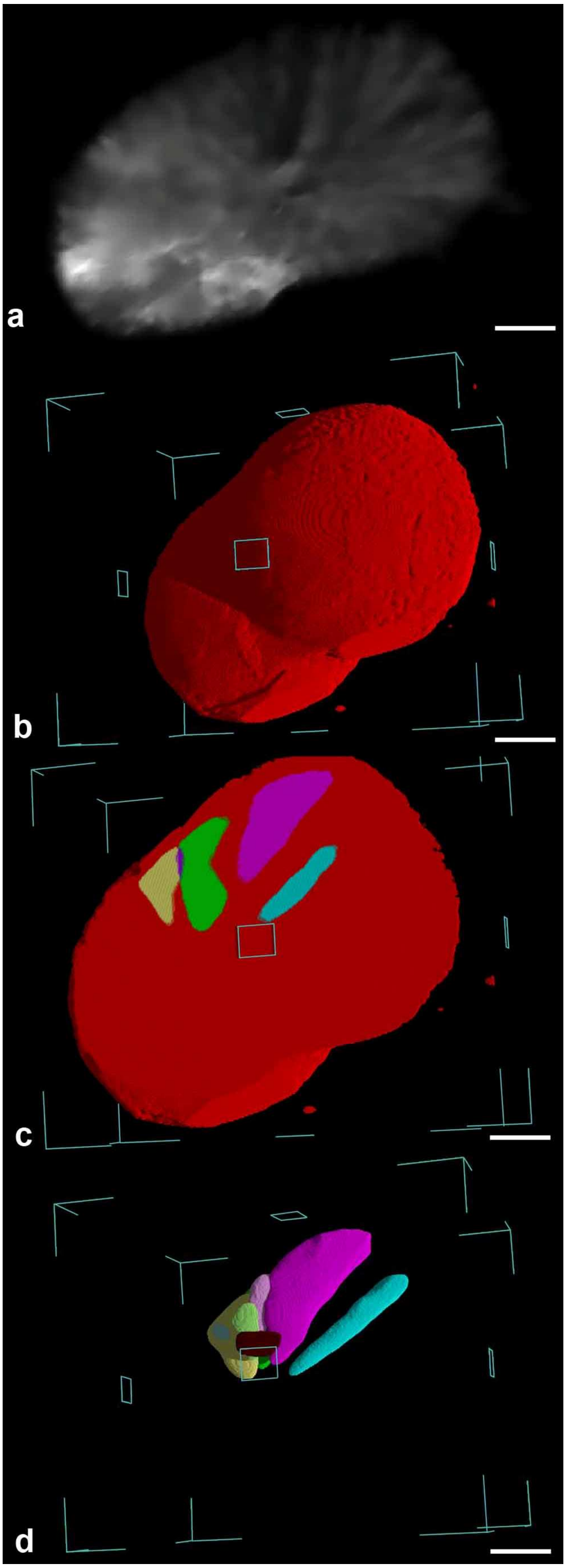

Fig. 8: *Chironex fleckeri*: **a** Diffraction topograph of main crystal **b-d** Diffraction-CT images, the colour code represents the individually identified crystals **b** complete statolith **c** cut

through the complete statolith **d** small crystals within the central part of the statolith, scale bars 100 µm.

Discussion

The recent discussion of the systematic order of the Cubozoa is based to date on classical morphological and histological features and some molecular data. The present investigation mainly focussed on detailed examinations of the statocysts and statoliths of the coronate scyphozoan medusa *P. periphylla* and of the chirodropide cubozoan medusa *C. fleckeri*. Additionally some classical morphological and anatomical features were examined for the comparison with other rhopaliophoran species. The statolith is part of the gravity-sense of the rhopaliophoran medusa and thus important for the organism orientation. Hence the statolith should be a conservative characteristic that could be changed only while preserving its function. Therefore, the statolith appeared to be a good target for the examination of phylogenetic relationships, especially in combination with new and sophisticated methods, such as SRµ-CT. Examinations of statoliths using light microscopy and scanning electron microscopy used in previous studies provides only information regarding the shape and surface of the statoliths as well as images of an artificially-prepared cut surface within the crystal. Sophisticated methods used in the present study such as X-ray single crystal diffraction analysis, microcomputer tomography (µ-CT) and X-ray diffraction imaging using a synchrotron beam line have the advantage of providing a non-destructive and undisturbed view inside of the statocyst and even inside the crystal, as well as providing information on statolith composition.

The x-ray single crystal diffraction is a common technique used to identify minerals and to clarify their detailed crystal structure as well as the atomic spacing, including bond-lengths, bond-angles and site-ordering information. Results of this technique have shown that the statolith of the *C. fleckeri* medusae was composed of the comparably rare (in the animal kingdom) biomineral, bassanite (calcium sulfate hemihydrate) as it is occurs only in other scyphozoans and cubozoans (Becker et al. 2005, Boßelmann et al. 2007, Tiemann et al. 2002, Tiemann et al. 2006). The structural parameters of the trigonal cell unit were refined to unit cell dimensions a = 6.95150(10), b = 6.95150(10) and c = 6.3516(3) Å in good agreement with the literature values of a = 6.937 and c = 6.345 Å for bassanite (Abriel and Nesper 1993). Even though the statolith appears as one solid piece, it did not have a single crystal structure, because the crystal lattice of the sample was not continuous. It was, in contrast, composed of several individually recognizable oligocrystals.

Synchrotron-based computed microtomography (SRµCT) using hard X-rays is a useful method to distinguish between organic tissue and minerals located within this tissue because of the strong differences in their absorption of X-rays (Beckmann et al. 1999, Bonse et al. 1996, Neues et al. 2007, Tadic et al. 2004). The great advantage of this method is that it is non-destructive and cuts can be performed virtually on a three-dimensional dataset. This method has been used previously to show the location and orientation of statoliths within the statocysts of different scyphozoan species (Becker et al. 2005, Boßelmann et al. 2007, Prymak et al. 2005).

X-ray absorption and phase sensitive imaging techniques reveal differences in the local X-ray attenuation coefficient and in the electron density of the material, respectively. However, both techniques (X-ray single crystal diffraction and SRµ-CT) fail to image the grain structure in monophase poly- and oligocrystalline materials, since crystals of different orientation generally do not show any difference in material properties like electron density. Two-dimensional projection images of individual crystals can be obtained by a technique known as X-ray diffraction imaging ("topography") (Tanner 1976). Here we have employed an extension of the X-ray diffraction imaging method to three dimensions, termed X-ray diffraction contrast tomography (Johnson 2008, Ludwig et al. 2008, Ludwig et al. 2009). DCT is a synchrotron X-ray imaging technique combining the concepts of X-ray diffraction and tomographic imaging and provides access to the shape and crystallographic orientation of the grains in poly- and oligocrystalline materials as it occurred in *Chironex fleckeri* statoliths.

The organisation of the statocyst itself appears to be different within the Scyphozoa and Cubozoa. The statoliths are surrounded by gastrodermal cells in both examined species, but in *P. periphylla* the whole statocyst was filled with gastrodermis cells that contain the statoliths, which increase in number and grow independently, whereas in cubomedusae, a thin single-layer of gastrodermis was covering one large compact statolith, which show daily growth rings (Boßelmann et al. 2007, Claus 1878, Conant 1898, Gordon et al. 2004, Holst et al. 2007, Kawamura et al. 2003, Pollmanns and Hündgen 1981, Schäfer 1878, Spangenberg 1968, 1976, Russel 1970, Ueno et al. 1995, Ueno et al. 1997). Only the aberrant *Tetraplatia volitans* has saccular sense organs on the oral sides of the lappets with a single statolith (Ralph 1960). This species was determined in older publications to be a coronate scyphozoan, but the examination of the smaller and larger subunits of the nuclear ribosome show that it belongs to the hydrozoan taxon Narcomedusae (Collins et al. 2006, Ralph 1960). The latter will be supported by the non scyphozoan-like statolith structure (Horridge 1969, Ralph 1960, Singla 1975).

Aside from these differences in the organisation of the statocysts of both species, we found fundamental similarities regarding the structure of the statoliths themselves. Firstly, the statoliths of *C. fleckeri* are comprised of the same biomineral bassanite as were found in *P. periphylla* and all the other examined scyphozoan and cubozoan species (Tiemann et al. 2002, Tiemann et al. 2006, Becker et al. 2005, Boßelmann et al. 2007). This is a very specific characteristic: Calcium sulfate is a very rare biomineral (Vinnikow et al. 1981, Lowenstam and Weiner 1989) and calciumsulfate-hemihydrate is, to date, known only in medusae of the taxon Rhopaliophora, among the metazoans.

Additionally, there are similarities regarding the crystallographic structure of the statoliths. The statoliths of *P. periphylla* increase in number with the age of the medusa, which results also in an increased width of the whole statocyst. The length and width of each statolith increases also with the age of the medusa, shown on the size of the five largest crystals. The development mode of the statocyst is comparable to the development of the statocyst of the scyphozoan medusa *Rhizostoma octopus* (Holst et al. 2007). This lead to the conclusion that the statocyst of the scyphozoan medusa grows by producing new, small statoliths, which grow independently and continuously by precipitation of new bassanite layers during their lifetime. A similar precipitation of biomineral is described for the statolith of the Cubozoa. Several authors described, *via* light-microscope, growth rings in ground statoliths of *Carybdea rastoni* and *Chiropsella bronzei* described as *Chiropsalmus quadrigatus* (Gordon et al. 2004, Kawamura et al. 2003, Ueno et al. 1995, Ueno et al. 1997). These growth rings were not recognizable with single crystal diffraction or SRµ-CT, which made it likely that they are caused by embedded organic material, as is described for the biominerals in other taxa (Wilt and Ettensohn 2007).

The distribution of different-sized statoliths (crystals) of *P. periphylla* within the statocyst was shown by SRµ-CT. The depression area with the smallest crystals was defined as the origin area of the statoliths. New statoliths developed in the basal gastrodermal cells with active nuclei and with very small vacuoles (Figs.1, 6). The crystals increased in size by continuous precipitation of bassanite; therefore the largest (oldest) crystals were located in the apical periphery, whereas the smaller (younger) crystals were located more in the centre. We found that the centre of the V-shaped indentation of the *C. fleckeri* statolith was comparable to the origin area of the *P. periphylla* statoliths. The compact statolith of *C. fleckeri* enclosed in this area a collection of small oligocrystals that were overgrown by one large oligocrystal as shown by DCT. The flattened areas of the outer oligocrystal detected by SRµ-CT could be interpreted as cystal faces of the bassanite. The origin area is described by Gordon et al.

(2004) and Ueno et al. (1995) as the centre of the statolith. Growth rings, which are apparent in the area of the outer large crystal, cannot be differentiated in this area (Ueno et al. 1995). Additionally, examinations of very young medusae of *Carybdea* sp. (Carybdeidae) show that their statocysts also contain several hexagonal crystals similar to the statocysts of scyphozoan medusae. These crystals consolidate into a compact mass later during their further development (Tiemann et al. 2006).

Cubozoa and Scyphozoa are separated in two classes due to differences during medusa formation and due to morphological features of the polyp and the medusa (Werner 1976). Even though the arguments for establishing the class Cubozoa are endorsed by several authors (Arneson and Cutress 1976, Yamaguchi and Hartwick 1980), it is not accepted by all authors (Matsumoto 1995, Ruppert et al. 2004). Some authors assume a sister group relationship between the Stauromedusae and the Cubozoa based on ribosomal RNA Data and the assumption that follicle cells are unique within the Stauromedusae (Marques and Collins 2004). Examinations of gonads of the coronate medusa *P. periphylla*, however, show that follicle cells also exist in other scyphozoan taxa (Tiemann and Jarms 2010). Other authors suggest the Cubozoa as sister group of the Scyphozoa with common ancestors and have established the common taxon Rhopaliophora. Based on morphological and anatomical features they conclude that the Scyphozoa and Cubozoa have common ancestors and are sister groups, closer related to each other than to other cnidarians (Ax 1995, Schuchert 1993). Some authors even assume that the metamorphosis of the Cubozoa might be derived secondarily from a monodisc strobilation mode, because of regenerating polyp remnants after medusa development in *Carybdea marsupialis* (Straehler-Pohl 2009, Straehler-Pohl and Jarms 2005, Thiel 1966). As a result, the rhopalia of the Scyphozoa and Cubozoa have been suggested by several authors to be homologous and synapomorphic characteristics (Ax 1995, Schuchert 1993, Thiel 1966). A main reason for this conclusion is the equivalent developmental mechanisms seen during medusa formation, especially because the bases of the polyp tentacles develop into the rhopalia during strobilation (Scyphozoa) or metamorphosis, respectively (Cubozoa) (Arai 1997, Calder 1973, 1982, Hofmann et al. 1978, Laska-Mehnert 1985, Schuchert 1993, Stangl et al. 2002, Werner 1975, 1993, Werner et al. 1971).

The anatomy of the rhopalia of some scyphozoan and cubozoan medusae e.g. of the genera *Periphylla, Paraphyllina*, *Nausithoe*, *Chrysaora*, *Cotylorhiza*, *Aurelia*, *Carybdea* and *Tripedalia* have been examined by several authors (Berger 1900, Bigelow 1910, Claus 1878, Conant 1898, Hertwig and Hertwig 1878, Hesse 1895, Maas 1903, Pollmanns and Hündgen 1981, Russel 1970, Schewiakoff 1889, Schäfer 1878, Skogh et al. 2006, Vanhöffen 1900, 1902). In our study, the rhopalia of *P. periphylla* and *C. fleckeri* had a club-like shape. The rhopalium of *C. fleckeri* was the more compact and stunted, as is typical for cubozoans. The rhopalium of *P. periphylla* however, was longer, more slender and bore a hood, as is typical for scyphozoans. The anatomy of the rhopalia of both examined species corresponded with the anatomical structure of other rhopaliophoran species regarding the gastrodermal channel and the thick epidermis with an agglomeration of neurones in the bulb, as well as the position of the statocyst in the apical part. Also comparable in both species, was the distally and aborally located thickened mesogleoa of the statocyst that is described also by Conant (1898) and Vanhöffen (1902). This could have an important role in mechanical fixation of the statocyst on the base of the rhopalium.

The rhopalia are assumed to serve as equilibrium or gravity sensors also because of the close relationship between the hair-cell neurites (which serve as mechanoreceptors) and the statocyst (Horridge 1966, Hündgen and Biela 1982, Holtmann and Thurm 2001, Nakanishi et al. 2009, Spangenberg et al. 1994, Spangenberg et al. 1996, Tardent and Schmid 1972). As described for other rhopaliophoran species the statocysts in *P. periphylla* and *C. fleckeri* developed within a terminal cyst of the gastrodermis, located in an identical position in close contact to the proximally-located neuroepithelium of the apical area of the rhopalium (Conant

1898, Haeckel 1879, Hertwig and Hertwig 1878, Laska and Hündgen 1984, Maas 1903, Russel 1970, Schewiakoff 1889, Satterlie 2002, Satterlie and Nolen 2001, Vanhöffen 1902). Newer information about sensing in cnidarian rhopalia is often related to light perception and conduction whereas information about gravity-sensing is more restricted (Horridge 1969, 1971, Horridge and MacKay 1962, Hündgen and Biela 1982, Laska and Hündgen 1982, 1984, Nakanishi et al. 2009, Spangenberg 1991, Spangenberg et al. 1994, 1996). Therfore, the multilayered neuroepithelium has been connected to the development of eyes (Claus 1878, Ekström et al. 2008, Garm 2006, Martin 2004, O'Connor et al. 2009, Skogh 2006), but could also be involved in processing and transmitting information about specimen position (Nakanishi et al. 2009). This is even more likely because it developed in a similar manner in *P. periphylla* medusae, which lacks an eye.

Both examined species had (similar to other rhopaliophorans) two sensory epithelia, that could be connected to mechanosense reception in homologous positions on the distal and proximal side of their rhopalia. These sensory areas are partially described as touchplates in scyphozoans (Bigelow 1910, Chapman 1985, Claus 1878, Conant 1898, Hesse 1895, Horridge 1969, Nakanishi et al. 2009, Pollmanns and Hündgen 1981, Russel 1970, Thiel 1936). The functionality of gravity-sensing would have to be slightly different in the two taxa: On one hand a statocyst that was movable against the bulb of the rhopalium with a hood as counterpart in *P. periphylla* and on the other hand a rhopalium with an immotile attached statocyst that was movable against the stalk using the stalk itself or even the rhopaliar niche as counterpart in *C. fleckeri*. This led to the assumption that the statolith had, in both cases, an indirect role in gravity-sensing. Supporting this claim, at least in *Tripedalia*, is the lack of neurons contacting the crystal directly (Garm pers. communication).

The anatomical comparison of the *P. periphylla* and *C. fleckeri* rhopalia demonstrated a coincident organization overall. Furthermore, the crystallographic structure of the statoliths, in particular, supports the conclusion that the marginal sense organs in Scyphozoa and Cubozoa are homologous structures. This lead to the hypothesis that the Cubozoa are a highly developed group of the Rhopaliophora with roots connected to scyphozoan ancestors.

Acknowledgements

We are grateful to HASYLAB at DESY, Hamburg and ANKA, Karlsruhe as well as the European Synchrotron Radiation Facility in Grenoble (France) for generous allocation of beamtime. For technical assistance and reconstruction of the microtomography scans at DESY we thank Felix Beckmann and Julia Herzen. Paulina Kämpfe and Henning Urch we thank for assistance during image recording at DESY. For assistance in specimen collection, we thank Jamie Seymour of TASRU (JCU) and grants from the Lions Foundation, National Geographic, Australian Geographic, Cairns City Council, Cardwell City Council, Smart State QLD, JCUPRS & GRS and Rio Tinto.

References

Abriel W, Nesper R (1993) Determination of crystal structure of $CaSO_4(H_2O)_{0,5}$ by X ray diffraction and potential profile calculations (in German). Z Kristallogr 205(1):99-113

Adam H, Czihak G (1964) Arbeitsmethoden der makroskopischen und mikroskopischen Anatomie. Ein Laboratoriumshandbuch für Biologen, Mediziner und technische Hilfskräfte. Fischer, Stuttgart

Adler L, Röper M, Jarms G, Rothgänger M (2007) Erstnachweis einer fossilen Hydromeduse vom Typ der rezenten Aequoreidae (Hydrozoa, Cnidaria) in den Plattenkalken von Painten. Acheopteryx 25:15-20

Arai MN (1997) A functional biology of Scyphozoa. Chapman & Hall, London

Arneson AC, Cutress CE (1976) Life history of *Carybdea alata* Reynaud (1830) (Cubomedusae). In: Mackie GO (ed) Coelenterate ecology and behaviour. Plenum, New York, pp 227–236

Ax P (1995) Das System der Metazoa I-III. Fischer/Spektrum, Stuttgart/Heidelberg

Becker A, Sötje I, Paulmann C, Beckmann F, Donath T, Boese R, Prymak O, Tiemann H, Epple M (2005) Calcium sulfate hemihydrate is the inorganic mineral in statoliths of scyphozoan medusae (Cnidaria). Dalton Trans. 1, 1545–1550.

Beckmann F, Bonse U, Biermann T (1999) New developments in attenuation and phase-contrast microtomography using synchrotron radiation with low and high photon energies. Proc SPIE 3772:179–187

Berger EW (1900) Physiology and histology of the cubomedusae including Dr. F.S. Conants notes on the physiology.The Hohns Hopkins Press, Baltimore pp1-81

Bigelow RP (1910) A comparison of the sense organs in medusae of the family Pelagiidae. J Exp Zool 9(4):751-785

Boßelmann F, Epple M, Sötje I, Tiemann H (2007) Statoliths of calcium sulfate hemihydrate are used for gravity sensing in rhopaliophoran medusae (Cnidaria) In: Baeuerlein E (ed) Biomineralisation: Biological Aspects and Structure Formation. Wiley-VCH, Weinheim, pp. 261-272.

Bonse U, Busch F (1996) X-ray computed microtomography (μCT) using synchrotron radiation (SR). Prog Biophys Molec Biol 65:133–169

Cartwright P, Halgedahl SL, Hendricks JR, Jarrard RD, Marques AC, Collins AG, Liebermann BS (2007) Exceptionally preserved jellyfish from the Middle Cambrian. PLoS ONE 2(10): e1121.

Calder DR (1973) Laboratory observations on the life history of *Rhopilema verrilli* (Scyphozoa: Rhizostomeae). Mar Biol 21:109–114

Calder DR (1982) Life history of the cannonball jellyfish, *Stomolophus meleagris* L. Agassiz, 1860 (Scyphozoa, Rhizostomida). Biol Bull 162:149–162

Chapman DM (1985) X-ray microanalysis of selected coelenterate statoliths. J Mar Biol Assoc UK 65:617–627.

Claus C (1878) Untersuchungen über *Charybdea marsupialis*. Alfred Hölder, Wien pp 1-56

Coates MM (2003) Visual ecology and functional morphology of Cubozoa (Cnidaria). Integr Comp Biol 43:542-548

Collins AG (2002) Phylogeny of Medusozoa and the evolution of cnidarian life cycles. J Evol Biol 15:418–432

Collins AG, Bentlage B, Matsumoto GI, Haddock HD, Osborn KJ, Schierwater B (2006) Solution to the phylogenetic enigma of *Tetraplatia*, a worm-shaped cnidarian. Biol Lett 2: 120-124.

Conant FS (1898) The cubomedusae. Johns Hopkins University Morphological Monographs. The Johns Hopkins Press, Baltimore pp 1-61

Donath T, Beckmann F, Heijkants RGJC, Brunke O, Schreyer A (2004) Characterization of polyurethane scaffolds using synchrotron ratiotion based computed microtomography. SPIE: Developments in X-Ray Tomography IV. 5535:775-782.

Ekström P, Garm A, Pålsson J, Vihtelic TS, Nilsson D-E (2008) Immunohistochemical evidence for multiple photosystems in box jellyfish. Cell Tissue Res 333:115-124

Fraser JH (1968) Standardization of zooplankton sampling methods at sea. In: Zooplankton sampling, part II. UNESCO Press, Paris, pp 149–168

Garm A, Ekström P, Boudes M, Nilsson D-E (2006) Rhopalia are integrated parts of the central nervous system in box jellyfish. Cell Tissue Res 325:333-343

Gordon M, Hatcher C, Seymour J (2004) Growth and age determination of the tropical Australian cubozoan *Chiropsalmus* sp.. Hydrobiologia 530/531:339-345

Haeckel E (1879) Das System der Medusen. Erster Teil einer Monographie der Medusen.

Fischer, Jena
Hertwig O, Hertwig R (1878) Das Nervensystem und die Sinnesorgane der Medusen. FCW Vogel, Leipzig
Hesse R (1895) Über das Nervensystem und die Sinnesorgane von *Rhizostoma buvieri*. Tübinger Zoologische Arbeiten 1(4):85-130
Hofman DK, Neumann R, Henne K (1978) Strobilation, budding and initiation of scyphistoma morphogenesis in the rhizostome *Cassiopea andromeda* (Cnidaria: Scyphozoa). Mar Biol 47:161–176
Holst S, Sötje I, Tiemann H, Jarms G (2007) Life cycle of the rhizostome jellyfish *Rhizostoma octopus* (L.) (Scyphozoa, Rhizostomeae), with studies on cnidocysts and statoliths. Mar Biol 151:1695-1710
Holtmann M, Thurm U (2001) Variations of concentric hair cells in a cnidarian sensory epithelium (*Coryne tubulosa*). J Comp Neuro 432:550-563
Horridge GA (1966) Some recently discovered underwater vibration receptors in invertebrates. In: Barnes H (ed) Some contemporary studies in marine science. George Allen and Unwin Ltd, London, pp 395-405
Horridge GA (1969) Statocysts of medusae and evolution of stereocilia. Tissue & Cell 1(2): 341-353
Horridge GA (1971) Primitive examples of gravity receptors and their evolution. In: Solon AG, Melvin JC (eds) Gravity and the organism. The University of Chicago Press, Chicago pp203-221
Horridge GA, MacKay B (1962) Naked axons and symmetrical synapses in coelenterates. Quart J micr Sci 103(4):531-541
Hündgen M, Biela C (1982) Fine structure of the touch-plate in the scyphomedusan *Aurelia aurita*. J Ultrastruct Res 80: 178-184
Johnson G, King A, Gonclaves Honnicke M, Marrow J, Ludwig W (2008) J Appl Crystallogr 41:310
Kawamura M, Ueno S, Iwanaga S, Oshiro N, Kubota S (2003) The relationship between fine rings in the statolith and growth of the cubomedusa *Chiropsalmus quadrigus* (Cnidaria: Cubozoa) form Okinawa Island, Japan. Plankton Biol Ecol 50(2):37-42
Laska G, Hündgen M (1982) Morphologie und Ultrastruktur der Lichtsinnesorgane von *Tripedalia cystophora* Conant (Cnidaria, Cubozoa). Zool Jb Anat 108:107-123
Laska G, Hündgen M (1984) die Ultrastruktur des neuromuskulären Systems der Medusen von *Tripedalia cystophora* und *Carybdea marsupialis* (Coelentata, Cubozoa). Zoomorphol 104:163-170
Laska-Mehnert G (1985) Cytologische Veränderungen während der Metamorphose des Cubopolypen *Tripedalia cystophora* (Cubozoa, Carybdeidae) in die Meduse. Helgoländer Meeresunters 39:129–164
Ludwig W, Schmidt S, Mejdal Lauridsen E, Poulsen HF (2008) X-ray diffraction contrast tomography: a novel technique for three-dimensional grain mapping of polycrystals. I. Direct beam case J Appl Cryst 41:302–309
Ludwig W, Reischig P, King A, Herbig M, Lauridsen EM, Johnson G, Marrow TJ, Buffiere JY (2009) Three-dimensional grain mapping by X-ray diffraction contrast tomography and the use of Friedel pairs in diffraction data analysis. Review of Scientific Instruments 80(3):033905–9.
Lowenstam HA, Weiner S (1989) On Biomineralization. Oxford University Press, New York
Martin VJ (2004) Photoreceptors of cubozoan jellyfish. Hydrobiologia 530/531:135-144
Marques AC, Collins AG (2004) Cladistic analysis of Medusozoa and Cnidarian evolution. Invertebr Biol 123(1): 23–42.
Matsumoto GI (1995) Observations on the anatomy and behaviour of the cubozoan *Carybdea rastonii* Haacke. Mar Fresh Behav Physiol 26:139-148

Maas O (1903) Die Scyphomedusen der Siboga Expedition. In: Weber, M (ed) Siboga-Expeditie XI, EJ Brill, Leiden pp 1-91

Mirone A, Wilcke R, Hammersley A, Ferrero C (2009) PyHST – High Speed Tomographic Reconstruction, <http://www.esrf.eu/UsersAndScience/ Experiments/ TBS/SciSoft/>.

Nakanishi N, Hartenstein V, Jacobs DK (2009) Development of the rhopalial nervous system in *Aurelia* sp.1. (Cnidaria, Scyphozoa). Dev Genes Evol 219:301-317

Neues F, Beckmann F, Ziegler A, Epple M (2007) The application of synchrotron radiation-based micro-tomography in biomineralization. In: Baeuerlein E (ed) Biomineralisation: Biological Aspects and Structure Formation. Wiley-VCH, Weinheim, pp. 369-380

O'Connor M, Garm A, Nilsson D-E (2009) Structure and optics of the eyes of the box jellyfish *Chiropsella bronzie*. J Comp Physiol A 195:557-569

Péron F, Lesueur CA (1809) Histoire générale et particuliére de tout les animaux qui composent la famille des Méduses. Ann Mus Hist Nat Marseille 14:316-366

Pollmanns D, Hündgen M (1981) Licht- und elektronenmikroskopische Untersuchung der Rhopalien von *Aurelia aurita* (Scyphozoa, Semaeostomae). Zool Jb Anat 105:508–525

Prymak O, Tiemann H, Sötje I, Marxen J, Klocke A, Kahl-Nieke B, Beckmann F, Donath T, Epple M (2005) Application of synchrotron radiation-based computer microtomography (SRµCT) to biominerals: embryonic snails, statoliths of medusae, and human teeth. J Bio Inorg Chem 10:688–695

Rack A, Weitkamp T, Bauer Trabelsi S, Modregger P, Cecilia A, dos Santos Rolo T, Rack T, Haas D, Simon R, Heldele R, Schulz M, Mayzel B, Danilewsky AN, Waterstradt T, Diete W, Riesemeier H, Müller BR, Baumbach T (2009) The micro-imaging station of the TopoTomo beamline at the ANKA synchrotron light source. Nucl Instr Phys Res B 267(11):1978-1988.

Ralph PM (1960) *Tetraplatia*, a coronate scyphomedusan. Proc Royal Soc London B 152 :263-281

Robinson DG, Ehlers U, Herken R, Herrmann B, Mayer F, Schürmann F-W (1985) Präparationsmethodik in der Elektronenmikroskopie. Eine Einführung für Biologen und Mediziner. Springer, Berlin, pp 1-208

Rupert EE, Fox RS, Barnes RD (2004) Cnidaria. In: Thomson (ed) Invertebrate zoology—a functional evolutionary approach. Brooks Cole, Belmont, pp 111–180

Russell FS (1970) The medusae of the British Isles. J Mar Biol Ass UK 39:303-317.

Salvini-Plawen L (1978) On the origin and evolution of the lower metazoa. Z Zool Syst Evol Forsch 16:40–88

Satterli RA (2002) Neuronal control of swimming in jellyfish: a comparative story. Can j Zool 80:1654.1669

Satterli RA, Nolan TG (2001) Why do cubomedusae have only four swim pacemakers? J Exp Biol 204:1413-1419

Schäfer EA (1878) Observations o the nervous system of *Aurelia aurita*. Phil Trans Royal Soc London 169:563-575

Schewiakoff W (1889) Beiträge zur Kenntnis des Acalephenauges .Morphol Jb 15:21-60

Schuchert P (1993) Phylogenetic analysis of the Cnidaria. Z Zool Syst Evol Forsch 31:161-173

Singla CL (1975) Statocysts of Hydromedusae. Cell Tissue Res. 158:391–407.

Skogh C, Garm A, Nilsson D-E, Ekström P (2006) Bilaterally symmetrical rhopalial nervous system of the box jellyfish *Tripedalia cystophora*. J Morphol 267:1391-1405

Southcott RV (1956) Studies on Australian Cubomedusae, including a new genus and species

apparently harmful to man. Australian Journal of Marine and Freshwater Research 7(2):254–280.
Spangenberg DB (1968) Recent studies of strobilation in jellyfish. Oceanogr Mar Biol Ann Rev 6:231–247
Spangenberg DB (1976) The mechanisms of mineralization in the invertebrates and plants. In: Watabe N, Wilbur KM (eds) University of South Carolina Press, Columbia pp231-248
Spangenberg D (1991) Rhopalium development in *Aurelia aurita* ephyrae. Hydrobiologia 216/217:45-49
Spangenberg DB, Beck CW (1968) Calcium sulfate dihydrate statoliths in *Aurelia*. Trans Am Microsc Soc 87 (3):329–335.
Spangenberg DB, Jernigan T, Philput C, Lowe B (1994) Graviceptor development in jellyfish ephyrae in space and on earth. Adv Space Res 14(8):317-325
Spangenberg DB, Coccaro E, Schwarte R, Lowe B (1996) Touch-plate and statolith formation in graviceptors of ephyrae which developed while weightless in space. Scan Microsc 10(3):875-888
Straehler-Pohl I (2009) Die Phylogenie der Rhopaliophora (Scyphozoa und Cubozoa) und die Paraphylie der „Rhizostomeae“. Doctoral Thesis University of Hamburg, Faculty of Mathematics, Informatics and Natural Sciences.
Straehler-Pohl I, Jarms G (2005) Life cycle of *Carybdea marsupialis* Linnaeus, 1758 (Cubozoa, Carybdeidae) reveals metamorphosis to be a modified strobilation. Mar Biol 147:1271-1277
Stangl K, Salvini-Plawen L v, Holstein TW (2002) Staging and induction of medusa metamorphosis in *Carybdea marsupialis* (Cnidaria, Cubozoa). Vie Milieu 52(4):131–140
Tadic D, Beckmann F, Donath T, Epple M (2004) Comparison of different methods for the preparation of porous bone substitution materials and structural investigations by synchrotron (micro)-computer tomography Mat-wiss u Werkstofftech 35:240–244
Tanner BK (1976) X-ray Diffraction Topography. Oxford: Pergammon.
Tardent P, Schmid (1972) Ultrastructur of mechanoreceptors of the polyp *Coryne pintnere* (Hydrozoa, Athecata). Exp Cell Res 72(1):265-275.
Thiel ME (1936) Scyphomedusae. In: Bronns HG (ed) Klassen und Ordnungen des Tierreichs. Akademische Verlagsgesellschaft, Leipzig
Thiel H (1966) The evolution of Scyphozoa. A review. In: The Cnidaria and their evolution. Symp Zool Soc Lond. Academic Press, London. 16:77-117
Tiemann H, Sötje I, Jarms G, Paulmann C, Epple M, Hasse B (2002) Calcium sulphate hemihydrate in statoliths of deep-sea medusae. J Chem Soc, Dalton Trans 1266–1268
Tiemann H, Sötje I, Becker A, Jarms G, Epple M (2006) Calcium sulfate hemihydrate (bassanite) statoliths in the cubozoan *Carybdea* sp.. Zool Anz 245:13–17
Tiemann H, Jarms G (2010) Organ-like gonads, complex oocyte formation, and long-term spawning in *Periphylla periphylla* (Cnidaria, Scyphozoam, Coronatae). Mar Biol 157:527-535
Ueno S, Imai C, Mitsutani A (1995) Fine growth rings found in statolith of a cubomedusa *Carybdea rastoni*. J Plankton Res 17(6):1381–1384.
Ueno S, Imai C, Mitsutani A (1997) Statolith formation and increment in *Carybdea rastoni* Haacke, 1886 (Scyphozoa: Cubomedusae): evidence of synchronization with semilunar rhythms. In: Proceedings of the 6th international conference on coelenterate biology: 491–496
Vanhöffen E (1900) Über Tiefseemedusen und ihre Sinnesorgane. Zool Anz 23:277-279
Vanhöffen E (1902) Die acraspeden Medusen der deutschen Tiefsee-Expedition 1898-1899. 3:1-49
Vinnikow YA, Aronove MZ, Kharkeevich TA, Tsirulis TP, Lavrowa EA, Natochin YV

(1981) Structural and chemical features of the invertebrate otoliths. Z mikrosk-anat Forsch 95: 127

Werner B (1973) New investigations on systematics and evolution of the class Scyphozoa and the phylum Cnidaria. Pub Seto Mar Biol Lab 20:35–61

Werner B (1975) Bau und Lebensgeschichte des Polypen von *Tripedalia cystophora* (Cubozoa, class, nov. Carybdeidae) und seine Bedeutung für die Evolution der Cnidaria. Helgoländer wiss Meeresunters 27:461–504

Werner B (1976) Die neue Cnidarierklasse Cubozoa. Verh Dtsch Zool Ges, p 230

Werner B (1993) Stamm Cnidaria, Nesseltiere. Lehrbuch der speziellen Zoologie. Kaestner A (ed) Fischer, Stuttgart. Vol. I/2: 11-305.

Werner B, Cutress EC, Studebaker JP (1971) Life cycle of *Tripedalia cystophora* Conant (Cubomedusae). Nature 232(5312):582–583

Wilt FH, Ettensohn CA (2007) The morphogenesis and biomineralization of the sea urchin larval skeleton. In: Bauerlein, E. (Ed.), Handbook of Biomineralization: Biological Aspects and Structure Formation, vol. 1. Wiley-VCH, pp. 183-210.

Yamaguchi M, Hartwick R (1980) Early life history of the Sea Wasp, *Chironex fleckeri* (Class Cubozoa). In: Tardent P, Tardent R (eds) Developmental and cellular biology of coelenterates. Elsevier/North-Holland Biomedical Press, Amsterdam, pp 11–16

Figure legends

Fig. 1: *Periphylla periphylla*: Longitudinal section of the rhopalium, median, photograph, scale bar 100 µm, e-epidermis, g-gastrodermis, gc-gastrovascular cavity, h-hood, m-mesogloea, n-neurons, np-neuropil, sa-sensory area, sg-statolith producing gastrodermis, sv-statolith vacuole (statoliths are dissolved during preparation).

Fig. 2: *Chironex fleckeri*: lightmicroscopical photograph of a complete fixated (90 % ethanol) rhopalium, paramedian view, scale bar 100 µm, l-lense, lle-lower lens eye, m-mesogloea, pl-pigment layer, sk-stalk, se-slit eye, st-statolith, ule-upper lens eye.

Fig. 3: *Chironex fleckeri*: Longitudinal section of the rhopalium, median, diagram, scale bar 100 µm, the gastrovascular channel within the stalk is not shown, b-balloon cells, l-lens, e-epidermis, g-gastrodermis, gc-gastrovascular cavity, m-mesogloea, n-neurons, np-neuropil, pl-pigment layer, rs-rhopalial stalk, sa-sensory area, sg-statolith producing gastrodermis, ds-dissoved statolith , vl-vitrous layer.

Fig. 4: Diagram of a longitudinal section through a rhopalium.
a *Periphylla periphylla*, scale bar 50 µm **b** *Chironex fleckeri* scale bar 200 µm
e-epidermis, g-gastrodermis, gc-gastrovascular cavity, h-hood, le-lens eye with retina, m-mesogloea, n-neuropil, rl- retinal layer, rn-rhopalial niche, sa-sensory area, sc-statocyst with statolith(s), rhopalium position (arrow cross): ao-aboral, d-distal, o-oral, p-proximal.

Fig. 5: *Periphylla periphylla*. **a** Increasing statocyst width in relation to medusa diameter, examined individuals N=56, **b** Increasing statolith number in relation to medusa diameter, examined individuals N=43, **c** Increasing statolith width in relation to medusa diameter, examined individuals N=45.

Fig. 6: *Periphylla periphylla*: Microtomography of statoliths of two statocysts from different sized medusae, **a-c** CD medusa 8.4 mm, **d-e** CD medusa 55 mm, **a-e** figures of the complete accumulation of statoliths of a statocyst, **a+e** side view, **b+e** view on the basal area containing the smallest statoliths, **c+f** longitudinal cut section through the reconstructed statocysts, arrows: basal area containing the smallest statoliths, scale bars = 100 µm.

Fig. 7: *Chironex fleckeri*: Microtomography. **a** complete statolith, the lower side is directed towards the stalk (basally) **b** cut section through the reconstruction of the short axis of the statolith, scale bars 100 µm

Fig. 8: *Chironex fleckeri*: **a** Diffraction topograph of main crystal **b-d** Diffraction-CT images, the colour code represents the individually identified crystals **b** complete statolith **c** cut through the complete statolith **d** small crystals within the central part of the statolith, scale bars 100 µm.